Pergamon
www.elsevier.com/locate/asr

Adv. Space Res. Vol. 29, No. 11, pp. 1731–1740, 2002

0273-1177/02 $22.00 + 0.00
PII: S0273-1177(02)00086-8

THE INDIAN OCEAN EXPERIMENT: AEROSOL FORCING OBTAINED FROM SATELLITE DATA

K. Rajeev[1] and V. Ramanathan[2]

[1]*Space Physics Laboratory, Vikram Sarabhai Space Centre, Trivandrum 695 022, India*
[2]*Center for Atmospheric Sciences, Scripps Institution of Oceanography, University of California, San Diego CA 92093, USA*

ABSTRACT

The tropical Indian Ocean provides an ideal and unique natural laboratory to observe and understand the role of anthropogenic aerosols in climate forcing. Since 1996, an international team of American, European and Indian scientists have been collecting aerosol, chemical and radiation data from ships and surface stations, which culminated in a multi-platform field experiment conducted during January to March of 1999. A persistent haze layer that spread over most of the northern Indian Ocean during wintertime was discovered. The layer, a complex mix of organics, black carbon, sulfates, nitrates and other species, subjects the lower atmosphere to a strong radiative heating and a larger reduction in the solar heating of the ocean. We present here the regional distribution of aerosols and the resulting clear sky aerosol radiative forcing at top-of-atmosphere (TOA) observed over the Indian Ocean during the winter months of 1997, 1998 and 1999 based on the aerosol optical depth (AOD) estimated using NOAA14-AVHRR and the TOA radiation budget data from CERES on board TRMM. Using the ratio of surface to TOA clear sky aerosol radiative forcing observed during the same period over the Indian Ocean island of Kaashidhoo (Satheesh and Ramanathan, 2000), the clear sky aerosol radiative forcing at the surface and the atmosphere are discussed. The regional maps of AVHRR derived AOD show abnormally large aerosol concentration during the winter of 1999 which is about 1.5 to 2 times larger than the AOD during the corresponding period of 1997 and 1998. A large latitudinal gradient in AOD is observed during all the three years of observation, with maximum AOD in the northern hemisphere. The diurnal mean clear sky aerosol forcing at TOA in the northern hemisphere Indian Ocean is in the range of -4 to –16 Wm^{-2} and had large spatio-temporal variations while in the southern hemisphere Indian Ocean it is in the range of 0 to $-6Wm^{-2}$. The importance of integrating in-situ data with satellite data to get reliable picture of the regional scale aerosol forcing is demonstrated.

INTRODUCTION

The contribution of aerosols in regulation and redistribution of incoming solar radiation is well-recognised (Charlson et al., 1992). On a global average, this aerosol radiative forcing is of magnitude comparable with that due to the greenhouse gases, but with opposite sign. Due to the relatively shorter lifetime of aerosols in the troposphere (of the order of a week) they show large spatial variations in their physical and chemical properties and are predominantly regionally distributed. This aerosol radiative forcing comes through the scattering of the incoming solar radiation back to space and thereby increasing the albedo of the earth-atmosphere system (the direct effect) and by participating in the cloud processes wherein the aerosols act as the cloud condensation nuclei, thereby increasing the reflectivity and lifetime of clouds (the indirect effect). Presently, large uncertainties exist in the estimates of both the direct and indirect effect of aerosols on the climate forcing.

During the winter months, a large and persistent flow of continental (polluted) air mass into the Tropical Indian Ocean occurs by the northeasterly winds. The location of the Inter Tropical Convergence Zone (ITCZ) in the Indian Ocean during this period is generally at the south of the equator. These give rise to the large horizontal transport of the aerosol-laden airmass from the relatively dry continental areas to the deep ocean traversing different meteorological (cloud) regimes. This provides an ideal laboratory to observe and understand the role of anthropogenic aerosols in climate forcing (Ramanathan *et al.*, 1995). The Indian Ocean Experiment (INDOEX) was aimed at utilising this unique natural laboratory to study the long-range transport of trace species and aerosols from urban regions and assessing their direct and indirect radiative forcing. Extensive measurements of physical, chemical and optical properties of aerosols over the Indian Ocean based on surface, shipborne and aircraft platforms were conducted during the First Field Phase (FFP : February – March of 1998) and Intensive Field Phase (IFP : January – March of 1999) of INDOEX. The measurements of physical, chemical and optical properties of aerosols made during the INDOEX-FFP were used to develop a model of aerosol size distribution and single scattering albedo (Satheesh *et al.* 1999). This aerosol model is consistent with the measurements made during the INDOEX-IFP.

The main objectives of the present study are : (1) estimation of the regional aerosol optical depths (at 630 nm) based on the NOAA14-AVHRR data, (2) Estimation of the clear sky aerosol radiative forcing at the top-of-atmosphere (TOA) by combining spaceborne measurements of aerosol optical depth (AOD) and earth's shortwave (SW) radiation budget, and (3) Estimation of the clear sky aerosol forcing at the surface and within the atmosphere by combining the observed TOA clear sky aerosol forcing and the ratio of the surface to TOA clear sky aerosol forcing observed over the Kaashidhoo Climate Observatory (KCO : 4.96°N, 73.46°E) reported by Satheesh and Ramanathan (2000). The interannual and monthly variations of these parameters are presented. The study focus on the January – March period of 1997, 1998, and 1999 over the geographical area of 25°S-25°N, and 40°E-100°E. The SW flux (in the wavelength range of 0.3 – 5.0 μm) at TOA used here is from the observation of CERES on board TRMM satellite. The study also demonstrates the potential of satellite based measurements alone to estimate the TOA aerosol forcing. Though the satellite measurements are limited to the TOA aerosol forcing, combining them with the surface measurements yields the much needed forcing at the surface and within the atmosphere. It may be noted that while the TOA aerosol forcing gives the total radiation lost to space for the earth-atmosphere system, it is the distribution of the radiative forcing at the surface and within the atmosphere which is controlling the changes in the surface and atmospheric winds and temperatures. However, the present study is limited to only the clear sky conditions.

DATA AND METHOD OF ANALYSIS

AOD at 630 nm from NOAA14-AVHRR data

AOD at 630 nm (± 50 nm) is obtained by inverting the radiance observed at channel 1 of NOAA14-AVHRR. The NOAA14-AVHRR global area coverage (GAC) data of the afternoon pass over the Indian Ocean area (in the latitude range 25°S to 25°N and the longitude range 40°E-100°E) during 1 January - 31 March of 1997, 1998, and 1999 is used here. The inversion scheme used to determine the AOD from AVHRR data is explained in detail in Rajeev et al. (2000). Retrieval of AOD is based on comparison of the observed satellite radiance at channel 1 with the look-up tables of modelled radiances generated using the discrete ordinate radiative transfer method for a plane parallel atmosphere (Stamnes et al., 1988) with 32 layers in vertical. This method accounts for the multiple scattering by aerosols and molecules and absorption due to aerosols, water vapour and ozone and the wind-dependent surface reflectance. Aerosols are assumed to be well mixed in the boundary layer (up to 1km) and the aerosol number density decreases exponentially with height above 1km with a scale height of 0.8km, which is inferred from the LIDAR images during the observation period (Satheesh et al., 1999). In order to minimise errors in the retrieval of AOD, we have used the data only from the anti-solar side of satellite scan.

The aerosol scattering phase function and single scattering albedo used in the retrieval are based on the aerosol model developed using observations of the chemical, microphysical, and optical properties of aerosols over the Indian Ocean during the winter months (Satheesh et al., 1999). The aerosol scattering phase function used here is the same as that shown in figure 1 of Rajeev et al. (2000). The column integrated single scattering

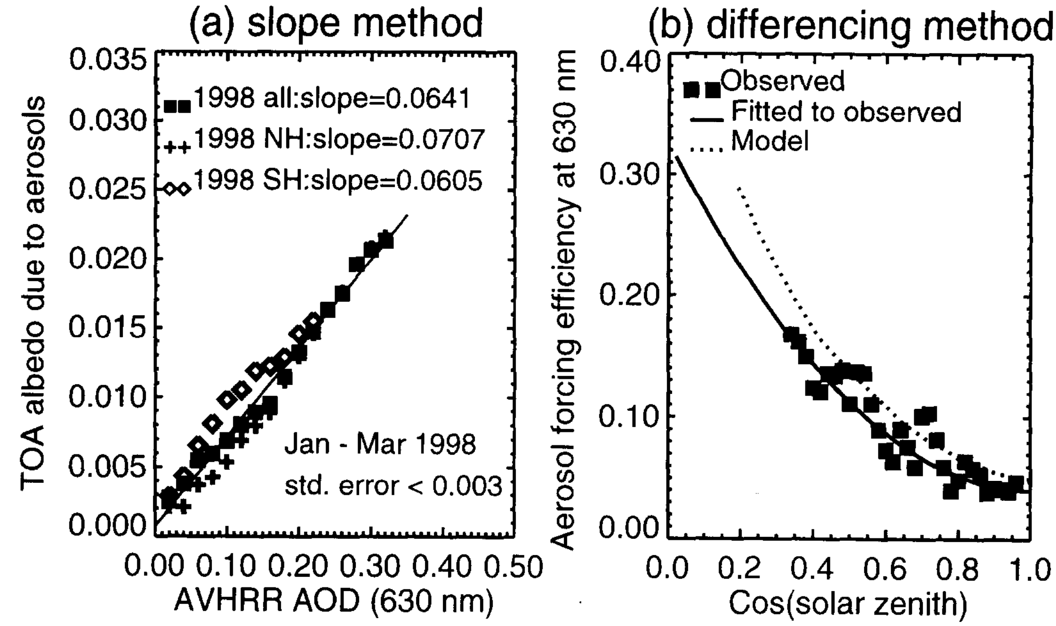

Fig.1. Estimation of clear sky aerosol forcing efficiency during January – March, 1998: (a) slope method, for $0.75<\mu<0.85$; (b) differencing method for all ranges of μ (After Rajeev and Ramanathan, 2001).

albedo used is 0.87. However, for very low optical depth (AOD < 0.15), the model accounts for non-absorbing component as explained in Rajeev et al. (2000). The satellite retrieved AOD is validated by comparing with in-situ observations as shown in Rajeev and Ramanathan (2000). The slope of the intercomparison is 0.977 and the mean bias is 0.020. The correlation coefficient is 0.921. The RMS deviation between the AVHRR and the in-situ AOD is 0.055. Based on the sensitivity analysis and the intercomparison of AVHRR AOD with the in-situ measured AOD, the typical uncertainty of the AVHRR derived AOD is approximately 15% (Rajeev and Ramanathan, 2000).

TOA shortwave flux from CERES

The shortwave flux (in the wavelength range of 0.3-5.0 μm) at the TOA is obtained based on the CERES measurements (Wielicki et al., 1996) on board TRMM. Pixel resolution of CERES onboard TRMM is 10 km at nadir. CERES observes the radiance in 3 spectral bands : the total spectral band (0.3μ - 200μm), the thermal spectral band (5μm - 200μm), and the window region (8μm - 12μm). The SW radiance is obtained by subtracting the observed radiance in the thermal band from that in the total band, and is converted to unfiltered SW radiance based on the instrument spectral characteristics. The SW radiance is converted to TOA SW flux using the ERBE-like inversion (Smith et al., 1986). This data set is referred as ERBE-like Science (ES-8) data, and it contains the instantaneous SW radiative fluxes at TOA for each CERES field of view. Here we have used the edition-2 of CERES-ES8 data set with the pixels identified as 'cloud free ocean'. The TOA SW fluxes are converted to TOA albedos by dividing by the instantaneous incident solar flux at the geographical location. The uncertainty in the instantaneous TOA albedo values is about 12.1%. The TOA latitude and longitude as given in CERES-ES8 data were converted to their surface values using the standard geometrical algorithm.

ESTIMATION OF CLEAR SKY AEROSOL FORCING EFFICIENCY

The clear sky aerosol forcing efficiency is estimated by collocating the AVHRR derived AOD with the CERES shortwave flux at the TOA and is explained in detail in Rajeev and Ramanathan (2000). Due to the precessing nature of the TRMM orbit, the time of observation of TOA albedo varies from day to day. The time of observation of AOD is nearly constant (approximately 1430 hrs local time during January-March 1998). In order to estimate the clear sky aerosol forcing efficiency at TOA, the mean AOD values for each latitude-longitude cell of grid size 0.2° in the geographical region of 25°N-25°S and 40°E-100°E, are collocated with the mean TOA albedo within a time interval of 2 hours for each day. However, the precessing nature of the TRMM orbit and the higher frequency of occurrence of cloud over the tropics limit the number of data points which are thus collocated. The study is made with values of collocated CERES broadband TOA albedo and the AVHRR AOD during the period 1 January - 31 March 1998 when sufficient number of collocated data points were available over the region. During 1999, the CERES data was available only during March 1999 (not continuous) due to operational problems with the satellite and the number of collocated data points available is too low compared to 1998. We used the 1999 data only for assessing the validity of the results obtained for the 1998 period.

Two methods are proposed for the estimation of clear sky aerosol forcing:(a) the slope method, and (b) the differencing method. The differencing method accounts for the variation of the aerosol forcing efficiency with solar zenith (θ) while the slope method is limited to a relatively smaller range of solar zenith angles.

In the slope method, the aerosol forcing efficiency (i.e., increase in TOA clear sky SW flux per unit increase in AOD at 630 nm) for a finite range of solar zenith angles is estimated by finding the slope of the variation of the aerosol contribution to TOA albedo with the AOD. In order to remove the solar zenith angle dependence of incoming solar flux, in this section the calculations are made in terms of albedo rather than flux. The aerosol contribution to the TOA albedo is obtained by subtracting the molecular contribution to albedo from total observed albedo at TOA observed by the satellite. The molecular contribution to the TOA albedo for a given range of μ (=cos(θ)) is computed based on the Monte Carlo model (Podgorny et al., 2000). However, in the present study, the slope method was limited to a range of $0.75<\mu<0.85$ because of the smaller number of collocated AOD and TOA albedo outside this range. The uncertainty in the model-calculated molecular contribution to the TOA albedo is typically about 5% in the solar zenith angle range of $0.75<\mu<0.85$. Figure 1(a) shows the variation of the aerosol contribution to the TOA albedo (averaged for AOD intervals of 0.02) with AOD. The mean value of μ is 0.80. The clear sky aerosol forcing efficiency at $\mu=0.80$ (in terms of albedo and for AOD of 630 nm) is given by the slope the least square fit to this variation (indicated by the straight line in Figure 1(a)) and is 0.0641. The intercept is 0.0007, which is very close to zero as expected. Figure 1(a) also shows the aerosol forcing efficiency for the northern (north of equator) and southern (south of equator) Indian Ocean. The aerosol forcing efficiency (i.e., the slope) for the northern and southern Indian Oceans are very similar and within the uncertainty limits. One of the main reasons is that the ITCZ is at about 5°S to 10°S and the anthropogenic aerosols extend to south of equator. Hence the data for the entire tropical Indian Ocean region is combined together, and the northern hemisphere and southern hemisphere are not treated separately for further calculations. As described earlier the maximum uncertainty in the TOA albedo is ~12.1% and that in the AVHRR retrieved AOD is ~15%. The two errors are not correlated. Thus, the uncertainty in the aerosol forcing obtained based on the above method is estimated to be about 20%. The aerosol forcing efficiency obtained from similar analysis for the March 1999 (number of collocated points are only 7585) is 0.0496 for $0.75\leq\mu\leq0.85$. The results are in agreement with in the uncertainty limits.

In order to find the diurnal mean clear sky aerosol forcing efficiency at TOA (f_d, which is the change in the diurnal mean clear sky short wave radiative flux at TOA with unit increase in AOD) the variation of the aerosol forcing efficiency with solar zenith is required, which is computed based on the differencing method. In this method, we have taken two ranges of AOD viz. (a) $0.0 \leq$ AOD ≤ 0.05 (with mean AOD of τ_{a1}) and (b) $0.15 \leq$ AOD ≤ 0.25 (with mean AOD of τ_{a2}) and the corresponding observed mean albedo (α_1 and α_2 for $0.0 \leq$ AOD $\leq$ 0.05 and $0.15 \leq$ AOD ≤ 0.25 respectively) for ranges of μ with bin size of 0.02 are calculated. The clear sky aerosol forcing efficiency (f_e) for each interval of μ is determined by taking the ratio of the difference between α_1 and α_2 (=$\Delta\alpha$) to the corresponding difference between τ_{a1} and τ_{a2} (=$\Delta\tau_a$). i.e., $f_e(\mu) = \Delta\alpha/\Delta\tau_a$. The variation of $f_e(\mu)$ as a function of μ thus calculated is shown in figure 1(b) using a solid square symbol. f_e increases with decrease in μ. The solid line in figure 1(b) shows the quadratic fitted to the observed forcing, given by $f_e(\mu)=a + b\mu + c\mu^2$, where a=0.3259, b=-0.5684, c=0.2825. The clear sky aerosol forcing based on the Monte Carlo model (Podgorny et al., 2000) is also shown in the figure 1(b) for comparison. The forcing efficiency obtained by the model shows very similar variation compared to the observed forcing, but is slightly larger than the observed values. The aerosol forcing efficiency at $\mu=0.80$ using the quadratic fit to the observed forcing in this method is

0.0519 while that obtained using the differencing method is 0.0641 which is 19% more than the former, but within the uncertainty limit of the derived forcing efficiencies (approx. 20%).

Because the differencing method gives the dependence of forcing efficiency as a function of μ which is essential for the estimation of the diurnal mean forcing efficiency and that the agreement between the slope method and the differencing method are within the limits of uncertainty, we have used the clear sky aerosol forcing efficiency obtained using the differencing method in the subsequent calculations. This method is applied only to 1998 data because the number of data points for most of the range bin of μ is insufficient during 1999 for the application of this method.

The diurnal mean clear sky aerosol forcing efficiency (f_d) on any given day is calculated by accounting for the instantaneous solar flux at any given geographical region and the μ dependence of aerosol forcing obtained by the differencing method, using the relation:

$$f_d = \frac{S_0}{2\pi}\left[\frac{d_0}{d}\right]^2 \int_{-h0}^{h0} \cos(\theta) f_e(\theta) d\theta \qquad (1)$$

where S_0 (=1367 Wm^{-2}) is the mean solar flux per unit area at the mean sun-earth distance (d_0) for the perpendicular beam with θ=0, d is the sun-earth distance on the given day of the year. h_0 is the hour angle at sunrise and sunset. Here f_d is expressed in terms of flux rather than albedo for better comparison with the values of f_d shown by other studies.

Figure 2 shows the variation of f_d (for AOD at 630 nm) with latitude and julian day. The value of f_d is in the range of 29 - 34 Wm^{-2}, and on most of the latitudes and days of observation f_d is close to 31 Wm^{-2}. The high value of f_d seen at the southernmost latitudes during January is because of the sun being at the southern hemisphere during this time resulting in higher solar flux and increased duration of the daytime. The uncertainty of f_d is approximately 20%, i.e., about 6 Wm^{-2}.

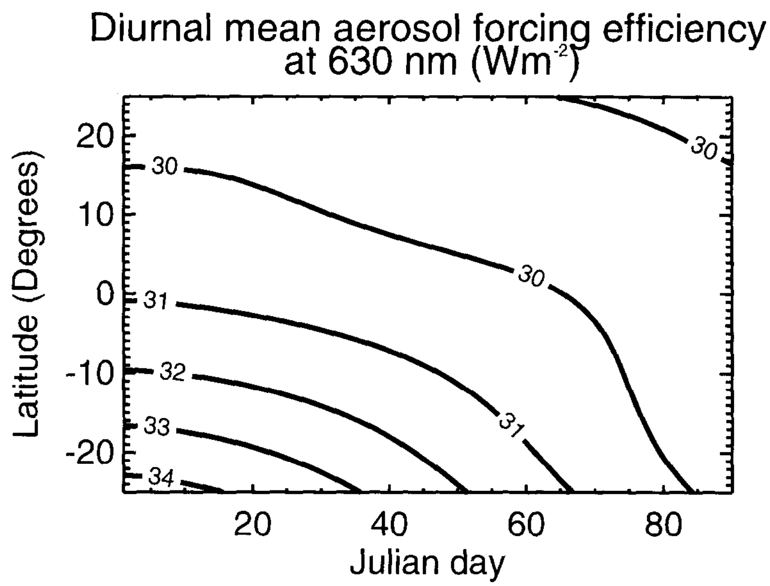

Fig.2. The diurnal mean clear sky aerosol radiative forcing efficiency at TOA, f_d, (for AOD at 630 nm) as a function of latitude and julian day (averaged in the longitude range of 50°E-100°E).

AEROSOL DISTRIBUTION AND CLEAR SKY ARESOL FORCING AT TOA

The diurnal mean clear sky aerosol forcing observed at the TOA is obtained by multiplying the observed AOD with the diurnal mean clear sky aerosol forcing efficiency. Plate 1 shows the regional distribution of the monthly and diurnal mean clear sky aerosol forcing at TOA over the Indian Ocean during January, February and March of 1997, 1998 and 1999. The regional distribution of aerosols is very similar to the regional distribution of clear sky aerosol forcing at TOA (since the TOA clear sky aerosol forcing is directly proportional to the AOD) and hence the AOD maps are not shown separately here.

Plate 1 shows that the aerosol concentration and the clear sky aerosol forcing are maximum in the northern hemisphere (NH) compared to the southern hemisphere throughout the observation period. The transport of aerosols from the continental land mass deep into the ocean areas is significant up to about 5°S. [The winds are predominantly northerly to north-easterly in the NH during the winter months in the lower troposphere (surface to 850 hpa) as seen from Rajeev et al., (2000)]. The AOD and the resulting clear sky aerosol forcing are maximum close to the continental boundaries of the Indian subcontinent, Southeast Asia and Arabia. Towards the south, the aerosol forcing is minimum around 5°S-10°S. This region of minimum AOD is associated with the ITCZ, where the aerosol removal is maximum due to rainout and washout processes. The large north-south gradient in the clear sky aerosol forcing across the northern boundary of ITCZ and in the northern hemisphere is remarkable over the all the longitudes. The aerosol loading increases slightly to the south of the ITCZ, though this increase is significantly smaller than that at the north of ITCZ. This increase in aerosol loading is aided by the increased lifetime of the aerosols at the south of ITCZ due to less efficient aerosol removal mechanisms. High wind speeds at about 20°S-25°S might also produce high amounts of sea salt aerosols. Further during some of the periods (particularly observed during 1998), large aerosol plumes originating in the continental areas in the northern hemisphere appears to penetrate deep into the southern hemisphere causing inter-hemispherical transport of aerosols. A combination of all these processes appears to have caused the increase in AOD at south of ITCZ.

The latitude variations of AOD (average for the latitude range of 50°E-100°E) during January, February, and March of 1997, 1998, and 1999 are shown in figure 3. The large north-south gradient in the aerosol loading is seen throughout the observation period. Higher AOD and latitude gradient in the Northern Hemisphere are observed during March compared to January and February during all the years of observation.

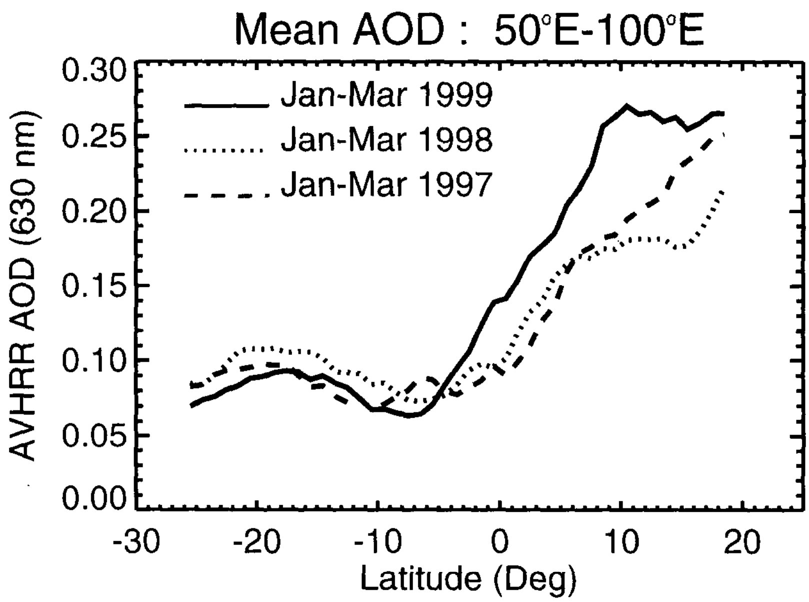

Fig.3. Seasonal mean latitude variation of AOD (averaged in the longitude range of 50°E-100°E during January – March) during 1997, 1998 and 1999.

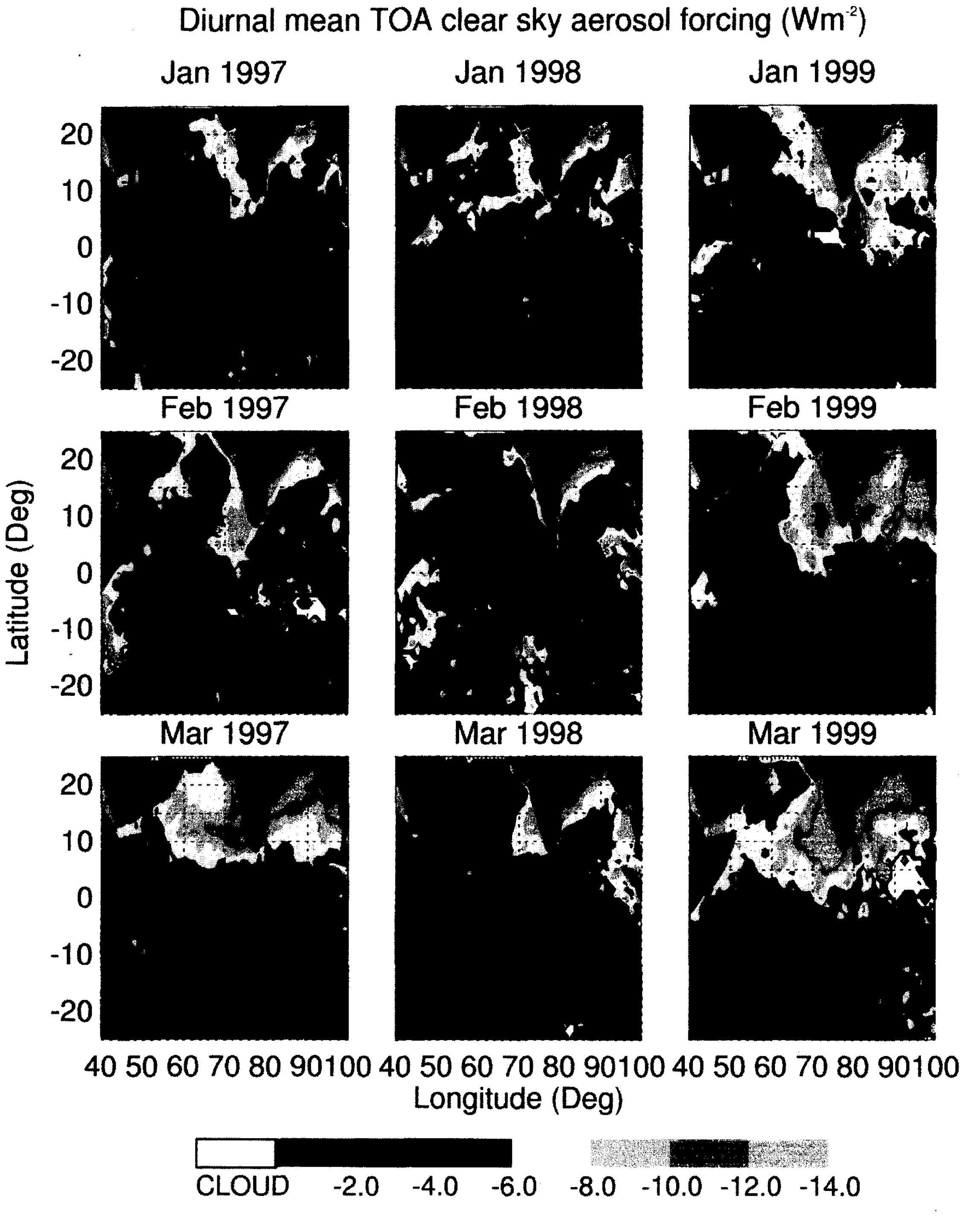

Plate 1. Regional TOA clear-sky aerosol radiative forcing during January, February and March of 1997, 1998 and 1999.

The clear sky aerosol forcing shows considerable monthly and yearly variations as seen from plate1. However, the geographical pattern observed during the whole period is remarkably consistent from year to year for the same month. Large aerosol forcing is observed over the northwest Bay of Bengal close to the coastal India throughout the observation period. The large aerosol transport from the southeast Asia (the Sumatra longitude region) into the south Bay of Bengal is seen throughout. The central Bay of Bengal is sandwiched between these two aerosol plumes. A plume of aerosols off the southwest coast of Indian peninsula appears during March of 1997, 1998, and 1999. The intensity of this plume is highest during March of 1999. The geographical structure of this plume occurring in March is remarkably consistent during all the three years of observation.

However, the aerosol abundance and the resulting clear sky aerosol forcing show large year to year variability. The highest clear sky aerosol forcing at the TOA is observed during March of 1999 (approximately 4 – 16Wm^{-2}). Near the Indian subcontinent and southeast Asia, the TOA clear sky aerosol forcing is in the range of -8 to -16 Wm^{-2}. The aerosol forcing during March of 1999 near the southwest coast of Indian peninsula is a factor of 1.5 - 2 higher than the corresponding values during 1997 and 1998. The enhanced aerosol forcing observed during 1999 is mostly limited to the northern hemisphere and is almost completely absent in the southern hemisphere. One of the main reasons of the large aerosol loading observed during 1999 could be because of the larger subsidence of air (stronger inversion and the resulting decrease in ventilation of the lowest region of the atmosphere) in the lower-middle troposphere during 1999 compared to 1998. During March, 1999 the surface wind speed was lower at the south Arabian Sea (close to the peninsular India where the high AOD was observed) compared to March, 1998. Several breaks were seen in the ITCZ during 1998 (which leads to inter-hemispherical transport of aerosols) while such breaks were not significant during 1999 (more effectively preventing the transport of northern hemispherical aerosol laden air to the south of ITCZ). These also might have aided the accumulation of aerosols near the peninsular India during March 1999. The yearly and monthly variations in AOD in the southern hemisphere are, generally, very small and the TOA clear sky aerosol forcing is in the range of 0 to -6Wm^{-2}.

CLEAR SKY AEROSOL FORCING AT SURFACE AND WITHIN ATMOSPHERE

The aerosol radiative forcing at the surface will be more than that observed at the TOA, mainly because of the absorption and redistribution of the incoming solar radiation within the atmosphere. Based on the surface measurements of global, direct and diffuse broadband radiation data, the TOA SW flux, and the in-situ measurements of AOD at Kaashidhoo Climate Observatory (KCO), Satheesh and Ramanathan (2000) have shown that the ratio of surface to TOA clear sky aerosol forcing (R) is 3.0 which is close to the value of R=3.4 given by Podgorny et al. (2000) using the Monte Carlo model incorporating the aerosol model developed over the Indian Ocean during the winter monsoon season. The value of R=3.0 may not be applicable over the entire Indian ocean because of the variations in the aerosol species and aerosol single scattering albedo. Here we have estimated the aerosol radiative forcing at the surface from the TOA forcing assuming R=3.0 as given by the direct observations of Satheesh and Ramanathan (2000), but limited to 5°S-15°S and 65°E-85°E, which is within approximately ±10° around KCO. Over this region not far away from Kaashidhoo, it is safe to assume that the value of R may not be significantly different from R=3.0 because the aircraft and ship measurements conducted over the Indian Ocean during INDOEX by various groups (Ramanathan et al., 1999) suggests similar aerosol properties with single scattering albedo similar to what is observed at Kaashidhoo, at least for regions north of 5°S. The difference between the surface forcing and the TOA forcing is the net radiative heating of the atmosphere due to the presence of aerosols, in contrast to the cooling effect due to aerosols at the surface. The main purpose of this calculation is to show the large magnitude of the surface and atmospheric clear sky aerosol forcing compared to the aerosol forcing at the TOA and to emphasize the importance of combining the satellite and in-situ observations for obtaining a clear picture of the aerosol radiative effects.

Plate 2 shows the TOA, atmosphere and surface clear sky aerosol forcing during March of 1999 (when the aerosol loading is highest) over the region 65°E-85°E and 5°S - 15°N. It may be noted that the clear sky aerosol forcing at surface is smaller than -18 Wm^{-2} over most of the regions in the NH, and about -30 to -48 Wm^{-2} close to the coastal boundary of the Indian subcontinent. Over KCO, Satheesh and Ramanathan (2000) reported that the clear sky aerosol forcing at surface is approximately -33 Wm^{-2} during March 1999. This is in agreement with -36 ± 7.2Wm^{-2} over KCO during March 1999 estimated in the present study. The atmospheric heating due to aerosols is estimated to be corresponding to approximately 12 to 32Wm^{-2} over the NH, and is approximately 20 to 32Wm^{-2} near the coast of Indian subcontinent. This large aerosol forcing at the TOA, surface and within the atmosphere and their spatial gradients may have a significant effect in altering the dynamics of the region by altering the radiation budget and modifying the temperature and pressure gradients as shown by Boucher et al. (1998).

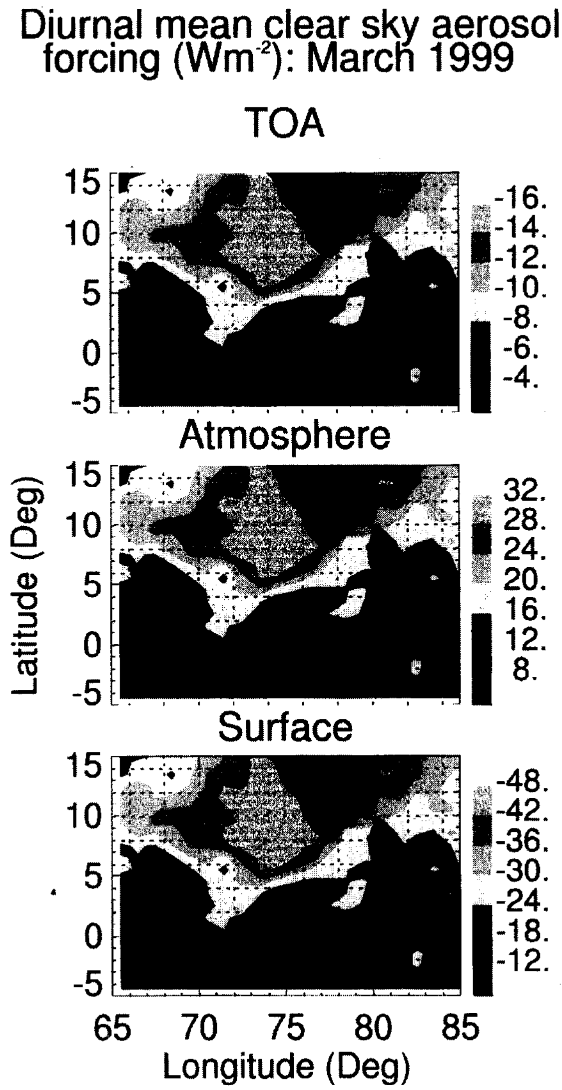

Plate 2. Estimated regional clear sky aerosol forcing at TOA, atmosphere, and surface during March of 1999

CONCLUSIONS

The regional distribution of aerosol optical depth (at 630 nm) over the Indian Ocean is derived using the radiance observed at channel 1 of NOAA14 AVHRR during January – March of 1997, 1998, and 1999. By combining the AVHRR derived AOD with TOA shortwave fluxes observed using CERES during January – March of 1998, we have derived the clear sky aerosol radiative forcing efficiency at TOA (i.e., increase in shortwave flux at TOA per unit increase in AOD at 630 nm). Using the regional distribution of AOD and the clear sky aerosol forcing efficiency, the regional clear sky aerosol forcing at the TOA over the Indian Ocean is derived. Assuming that the ratio of surface to TOA forcing is 3 as reported by Satheesh and Ramanathan (2000) during the same period of observation over the Indian Ocean island of Kaashidhoo, and using the observed clear sky aerosol forcing at the TOA, we have discussed the regional distribution of clear sky aerosol forcing at the surface and the atmosphere over a region within ±10° around Kaashidhoo.

This study demonstrates that in-situ and satellite data can be integrated to obtain the clear sky aerosol forcing directly from observations. Thus the results presented here provide an initial data set to integrate on climate models for regional clear sky aerosol radiative forcing. The main results of the present study are:

(1) During all the three years of observation, the over-all shape of the spatial distribution of the monthly mean aerosol loading is remarkably consistent, but with different magnitude of aerosol loading. Ocean areas in the entire Northern Hemisphere is affected by the large aerosol transport from the continental areas of the Indian subcontinent, Arabia and Southeast Asia. The aerosol loading at the northern hemisphere is about a factor of 2 to 5 larger than that at the south of ITCZ which results in the large latitude gradient in AOD observed at the northern boundary of ITCZ.

(2) One of the most striking feature of the present study is the abnormally large (by a factor of 1.5 to 2) aerosol loading over the northern Indian Ocean (north of ITCZ) during 1999 compared to 1997 and 1998. This increase in AOD during 1999 is observed both at the Bay of Bengal and Arabian Sea sectors, but is almost completely absent at the south of ITCZ. The decreased ventilation at the lower troposphere over the Indian subcontinent during 1999 might have played an important role in the increase in aerosol loading over the Indian Ocean.

(3) The clear sky aerosol forcing efficiency at TOA (for AOD at 630 nm) is estimated to be in the range 29 to 34Wm^{-2} over the Indian Ocean during the winter period. The clear sky aerosol forcing is significantly larger in the Northern Hemisphere (-4 to –16 Wm^{-2} at TOA) compared to the Southern Hemisphere (0 to -6 Wm^{-2} at TOA) during the entire observation period. These values are substantially higher than the global mean values reported in IPCC (1995) for sulfate aerosols alone.

(4) At the surface, the estimated clear sky aerosol forcing is very large (-12 to -48Wm^{-2}), and has very large spatio-temporal variations. The heating of the clear sky atmosphere due to aerosols is of the order of 8 to 32Wm^{-2}.

ACKNOWLEDGEMENTS

The CERES data is obtained from the NASA Langley Research Center EOSDIS Distributed Active Archive Center. We thank B. Barkstrom, B. A. Wielicki and K. J. Priestley for switching on the CERES sensors during the INDOEX-1999 operations. The authors thank B. Holben for providing aerosol optical depth measurements at Kaashidhoo Island in Maldives, which is part of AERONET. This study was funded by the National Science Foundation (NSF) through grant number ATM 9612887. The study was performed when one of the authors, K. Rajeev, was at Center for Clouds, Chemistry and Climate, Scripps Institution of Oceanography, UCSD, USA.

REFERENCES

Boucher, O., M. Pham, and R. Sadourny, General circulation model simulations of the Indian summer monsoon with increasing levels of sulphate aerosols, *Ann. Geophys.*, **16**, 346-352, 1998.

Charlson, R. J., S. E. Schwartz, J. M. Hales, R. D. Cess, J. A. Coakley, et al., Climate forcing by anthropogenic aerosols, *Science*, **255**, 423-430, 1992.

Intergovernmental Panel on Climate Change (IPCC), Climate Change, 1994: Radiative forcing of climate change and evaluation of IPCC IS92 emission scenarios, Edited by J. H. Houghton, 339 pp., Cambridge University Press, New York, 1995.

Podgorny, I.A., W. Conant, V. Ramanathan and S.K. Satheesh. Aerosol modulation of atmospheric and surface solar heating over the tropical Indian Ocean, *Tellus*, 52B, 947-958, 2000.

Rajeev, K., V. Ramanathan, and J. Meywerk, Regional aerosol distribution and its long range transport over the Indian Ocean, *J. Geophys. Res.*, **105**, 2029-2043, 2000.

Rajeev, K., and V. Ramanathan, Direct observations of clear-sky aerosol radiative forcing from space during the Indian Ocean Experiment, J. Gephys. Res., in press, 2001.

Ramanathan, V., et al., Indian Ocean Experiment (INDOEX) white paper, C4, Scripps Institution of Oceanography, University of California, San Diego, La Jolla, California, August, 1995.

Ramanathan, V., *et al.*, The Indian Ocean Experiment: An integrated analysis of the climate forcing and effects of the great Indian Ocean haze, *J. Geophys. Res.*, in press, 2001.

Satheesh, S. K., and V. Ramanathan, Large difference in tropical aerosol forcing at the top of the atmosphere and Earth's surface, *Nature*, *405*, 60-63, 2000.

Satheesh, S.K., V. Ramanathan, X. Li-Jones, J.M. Lobert, I.A. Podgorny, et al., A Model for the natural and anthropogenic aerosols over the tropical Indian Ocean derived from INDOEX data, *J. Geophys. Res.*, **104:**27, 421, 1999

Smith, G. L., R. N. Green, E. Rascheke, L. M. Avis, J. T. Suttles, et al., Inversion methods for satellite studies of the Earth radiation budget: Development of algorithms for the ERBE mission, *Rev. Geophys.*, **24**, 407-421, 1996.

Stamnes, K., S. –C. Tsay, W. Wiscombe, and K. Jayaweera, A numerically stable algorithm for discrete-ordinate-method radiative transfer in multiple scattering and emitting layered media, *App. Opt.*, **27**, 2502-2509, 1988.

Wielicki, B. A., et al., Clouds and Earth's Radiant Energy System (CERES): An Earth Observing System Experiment, *Bull. Amer. Meteor. Soc.*, **77**, 853-868, 1996.